ELSEVIER

Catalysis Today 68 (2001) 217–225

CATALYSIS TODAY

www.elsevier.com/locate/cattod

Nano-MgO: novel preparation and application as support of Ni catalyst for CO_2 reforming of methane

Bo-Qing Xu*, Jun-Mei Wei, Hai-Yan Wang, Ke-Qiang Sun, Qi-Ming Zhu

State Key Lab of C_1 Chemical Technology and Department of Chemistry, Tsinghua University, Beijing 100084, China

Abstract

A novel preparation method for MgO nanocrystals was reported. This new method makes use of a conventional hydrogel of $Mg(OH)_2$ derived from inorganic magnesium chloride. A change to alcogel of the hydrogel by repeated wash with anhydrous ethanol followed by processing the alcogel at elevated temperature with flowing dry nitrogen under normal pressure leads to a good control of the sizes of MgO nanocrystals (10–12 nm) that are able to resist "sintering" up to 650°C without significant loss of the surface area. This alcogel-based normal-pressure processing proved to be superior to the high-pressure alcogel-supercritical drying synthesis of the nanocrystals. Primary application of the MgO nanocrystals for support of nickel catalyst was successful and gave promising results for highly active as well as very stable Ni/MgO catalysts for the dry reforming of methane to produce syngas.

Keywords: MgO nanocrystals; Ni catalyst; Reforming of methane

1. Introduction

Magnesium oxide is an interesting basic oxide that has many applications. In the field of catalysis, MgO showed strongly basic property that associates with the base-catalysis in many organic reactions [1]. MgO is also an important support for metal catalyst, e.g., properly prepared nickel-supported MgO catalyst showed interesting anti-carbon ability in the reforming reaction of methane with CO_2 [2–4]:

$$CH_4 + CO_2 \rightarrow 2CO + 2H_2, \quad \Delta H = 247\,\mathrm{kJ/mol}$$

This is an important reaction in which two main green house gases are converted into desirable syngas for valuable fuels and chemicals [5]. Superior surface and catalytic properties are expectable when the MgO is synthesized as particles composed with small nanocrystals since they should have a high concentration of surface defects and a high ratio of edge ions/surface ions. The report by Ruckenstein and Hu [3] showed that NiO/MgO catalysts prepared by impregnation of nickel nitrate onto MgO powders containing 7–10 nm nanocrystals developed stable activities for the reforming reaction after reduction at 790°C.

It has been documented that methoxide or alkoxide-based sol–gel synthesis of metal hydroxides followed by supercritical drying and vacuum dehydration can lead to the formation of small nanocrystals or nanoparticles of metal oxides [6,7]. Usually, the alkoxide precursors are dissolved in an organic solvent and are transformed to metal hydroxides by adding a limited amount of water. The hydroxides thus formed are in their alcogels, which, followed by supercritical drying and dehydration at elevated temperature, are converted to the nanoparticles. Nanocrystals of MgO

---

* Corresponding author. Tel.: +86-10-6278-4589; fax: +86-10-6277-0304.
E-mail address: bqxu@tsinghua.edu.cn (B.-Q. Xu).

0920-5861/01/$ – see front matter © 2001 Elsevier Science B.V. All rights reserved.
PII: S0920-5861(01)00303-0

with an average size of ~4 nm was synthesized by use of $Mg(OCH_3)_2$ as a starting material [8–13]. Particulates based on these small MgO nanocrystals are shown to exhibit unexpectedly high surface chemical reactivities that have allowed their successful use as high capacity destructive adsorbents for toxic chemicals, including chlorocarbons, organophosphorus compounds, and acid gases like SO_2 [10–12].

For conventional catalytic application, the alkoxide-based synthetic approach could be expensive. A modification that avoids using of the organic salts (alkoxides) has been made, in which the alcogels were prepared by replacing with ethanol the water molecules within the hydrogel frameworks of metal hydroxide that are cheaply obtained from conventional inorganic salts [14–17]. For the preparation of ZrO_2, this modification has lead to the formation of 6–8 nm nanocrystals after drying an alcogel of zirconyl hydroxide under supercritical ethanol. Impregnation of nickel nitrate onto these nanocrystals of ZrO_2 followed by calcination and reduction of the nickel with hydrogen has developed extremely stable Ni catalysts for the production of syngas from methane and CO_2 [18–21].

In the present investigation, a further modification was made to avoid the use of the high pressure of supercritical ethanol for drying the alcogel of $Mg(OH)_2$ derived from inorganic $MgCl_2$. Instead, the $Mg(OH)_2$ alcogel is processed in flowing nitrogen under atmospheric pressure. By comparison with those from supercritical drying of the alcogel and from conventional processing of $Mg(OH)_2$ hydrogel in air, we show that this novel processing with atmospheric nitrogen can form small MgO nanocystals that are resistant to sintering up to 650°C.

Another motivation of this work is to test the potential of the novelly prepared MgO nanocryatals for developing highly active and anti-carbon nickel catalyst for the dry reforming of methane.

2. Experimental

2.1. Synthesis of $Mg(OH)_2$ and MgO nanocrystals

$MgCl_2\cdot 6H_2O$ of analytical grade (Beijing Shanhuan Chemical Reagent) was used as the precursor for preparing hydrogel of $Mg(OH)_2$ by sol–gel chemistry. Typically, to 500 ml aqueous solution of 0.4 M $MgCl_2$ was added drop-wise 2.5 wt.% aqueous ammonia (900 ml), while maintaining pH of the precipitating solution at ca. 9–10. The precipitated $Mg(OH)_2$ hydrogel gel was left to digest in the solution for 8 h at room temperature before it was separated by filtration and washed with doubly deionized water to be free of chlorine anions. One-third of the $Mg(OH)_2$ hydrogel was taken for drying in air at 110°C, which gave MgO-CP-110. The hydrogel was then calcined in air at 500 or 650°C; the samples thus prepared are coded as MgO-CP.

The remaining $Mg(OH)_2$ hydrogel was changed to alcogel by washing with anhydrous ethanol for several times. The resultant alcogel was divided into two parts. One part was placed in an autoclave. It was then pressurized (7.0 MPa) with dry nitrogen and was heated (ca. 5°C/min) to 270°C to form supercritical ethanol (243°C, 6.3 MPa). The autoclaved sample was allowed to experience drying under the supercritical ethanol for 1 h, followed by release of the pressure in flowing N_2 to cool the sample. To examine the sintering property, sample from the supercritical drying was further dehydrated by calcination in air to temperatures up to 650°C; samples thus obtained are coded MgO-AS. The second part of the alcogel was placed in a quartz tube reactor and dried/calcined to different temperatures up to 650°C (heating to 110°C at a rate of 2°C/min and then to the desired temperature at 5°C/min) in flowing N_2 under atmospheric pressure; samples prepared with this novel processing are named MgO-AN.

Properties of the $Mg(OH)_2$ and MgO nanocrystals obtained with the preparations described above are summarized in Table 1.

2.2. Preparation and catalytic testing of Ni/MgO catalyst

Samples of Ni/MgO were prepared by wet impregnation of an aqueous solution of $Ni(NO_3)_2\cdot 6H_2O$ onto nanocrystals of $Mg(OH)_2$ or MgO, depending on the support history which will be specified in Section 3, with a rotary evaporator. After drying at 110°C, the samples were calcined in air at 650°C for 5 h, and then stored for future use.

The catalytic reaction was conducted in a vertical fixed-bed U-shape quartz reactor (i.d. 10 mm) under atmospheric pressure. The catalyst bed contains

Table 1
Surface area and crystal size of $Mg(OH)_2/MgO$ prepared by different methods

Processing temperature (°C) [product code]	Alcogel precursor with supercritical drying (AS)		Alcogel precursor with drying/calcination in flowing N_2 (AN)		Conventional hydrogel precursor with drying/calcination in air (CP)	
	Crystal size (nm)	BET surface ($m^2 g^{-1}$)	Crystal size (nm)	BET surface ($m^2 g^{-1}$)	Crystal size (nm)	BET surface ($m^2 g^{-1}$)
110 [$Mg(OH)_2$-110]	–	–	–	–	11.2[a], 36.8[b]	49.7
270 [$Mg(OH)_2$-270]	14.6[a], 62.4[b]	58.2	10.5[a], 10.4[b]	52.4	–	–
350 [MgO-350]	–	–	11.7[c]	138.3	–	–
500 [MgO-500]	11.1[c]	165.3	11.5[c]	196.9	8.3[c]	105.3
650 [MgO-650]	17.0[c]	43.9	10.1[c]	97.6	22.0[c]	45.5

[a] Calculated from (0 0 1) diffraction line of $Mg(OH)_2$.
[b] Calculated from (1 1 0) diffraction line of $Mg(OH)_2$.
[c] Calculated from (2 0 0) diffraction line of MgO.

200 mg Ni/MgO that was diluted with 500 mg α-Al_2O_3. A capillary quartz tube (i.d. 1.5 mm) was inserted, from the exit side of the reactor, into the catalyst bed to introduce a thermal couple, which permits a measurement of the temperature at the catalyst bed. The catalytic reaction was performed at 757°C with a feed containing equal moles of CH_4 and CO_2. Unless otherwise specified, the flow rate of the feed was GHSV $= 2.4 \times 10^4\,ml/(h\,g_{cat})$. Before the reaction, the catalyst was reduced with a flow of 10% H_2/N_2 at 850°C for 3 h. Product analysis was performed on a GC with a GDX-50 as the separation column. The selectivity of CO was defined as the ratio, (moles of product CO)/(moles of converted CH_4 and CO_2); the ratio, (moles of product H_2)/(2(moles of converted CH_4)), gave the selectivity of H_2.

2.3. Characterization of $Mg(OH)_2$/MgO and Ni/MgO samples

The crystal structure of $Mg(OH)_2$/MgO and Ni/MgO samples were characterized with powder X-ray diffraction (XRD) on a Bruker D8 Advance X-ray Diffractometer using the Cu K2α source at 40 kV and 40 mA. The crystal size of MgO or $Mg(OH)_2$ was measured from the X-ray broadening by using the well-known Scherrer equation [22]:

$$d = \frac{0.089\lambda}{B(2\theta)\cos\theta}$$

where $B(2\theta)$ is the width of the XRD pattern line at half peak-height (rad), λ the wavelength of the X-ray, θ the angle between the incident and diffracted beams (°), and d the crystal size of the powder sample (nm).

Surface areas of the samples were measured with nitrogen adsorption at −196°C on a Chemsorb-3000 instrument. The samples were dehydrated with a flow of dry nitrogen at 180°C for 5 h before the adsorption measurement. TEM measurements of some samples were performed on a Hitachi H-800 electron microscope.

Quantitative temperature-programmed reduction (TPR) of the nickel-supported MgO was conducted up to 860°C and held at this temperature for 30 min on a homemade TPR apparatus with 5% H_2/Ar as the reductant. The temperature ramp was 15°C/min. Water, which is the only volatile product of the reduction reaction, was removed from the exit gas with a cold trap at −85°C to avoid its interference into the TCD detector. Before the reduction, the sample was cleaned with pure Ar at 600°C for 30 min. The TPR measurement was followed by a H_2-TPD to measure the chemisorption of hydrogen. The ratio of 2(area of TPD-peak)/(area of TPR-peak) gives the dispersion of the reduced nickel metal.

3. Results and discussion

3.1. Novel preparation of MgO nanocrystals with no supercritical drying

Fig. 1 shows the XRD pattern of the samples synthesized with different preparations. Starting from the alcogel of $Mg(OH)_2$, both the high-pressure

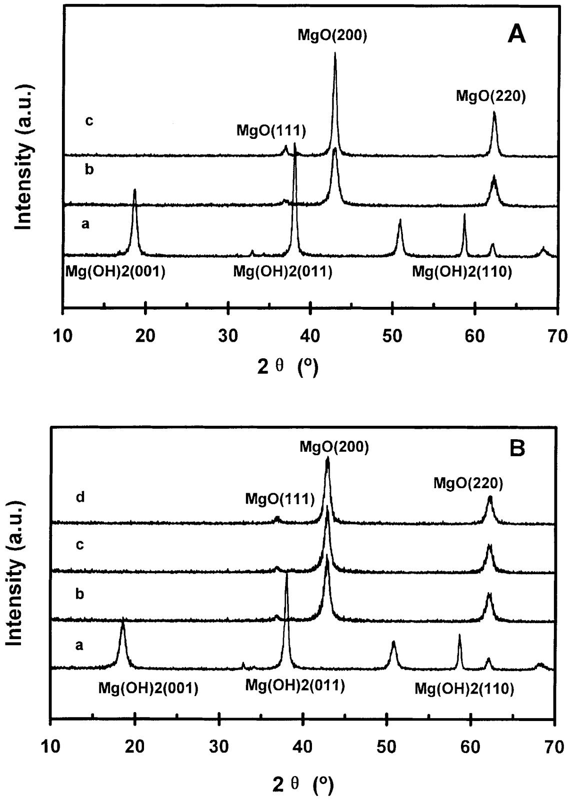

Fig. 1. XRD patterns of $Mg(OH)_2$ or MgO samples with different preparations: (A) high-pressure drying under supercritical ethanol of the $Mg(OH)_2$ alcogel followed by calcinations at 270 (a), 500 (b) and 650°C (c); (B) normal-pressure drying of the $Mg(OH)_2$ alcogel with flowing nitrogen at 270 (a), 350 (b), 500 (c) and 650°C (d).

supercritical drying (AS preparation) and the normal-pressure drying in nitrogen atmosphere (AN preparation) at 270°C produced nanocrystals of $Mg(OH)_2$ (Fig. 1). Though the surface areas of these two hydroxides after dehydration at 180°C are comparable, the shape and crystal sizes of these two samples are different (Table 1). The sample dried under supercritical ethanol produced elongate $Mg(OH)_2$-AS-270 nanocrystals with averaged dimensions of ca. 14 nm × 62 nm (14 nm in the direction of (0 0 1) planes and 62 nm in the direction of (1 1 0) ones), while the sample dried under the normal pressure produced near round $Mg(OH)_2$-AN-270 crystals averaged to ca. 10 nm. The TEM microgram shown in Fig. 2 confirms the elongate shape of the $Mg(OH)_2$-AS-270 nanocrystals. The conventional hydrogel preparation of the hydroxide also produced elongate nanocrystals (ca. 11 nm × 37 nm), $Mg(OH)_2$-CP-110 (Table 1); the TEM microgram of this sample was similar to Fig. 2, but showed smaller sizes.

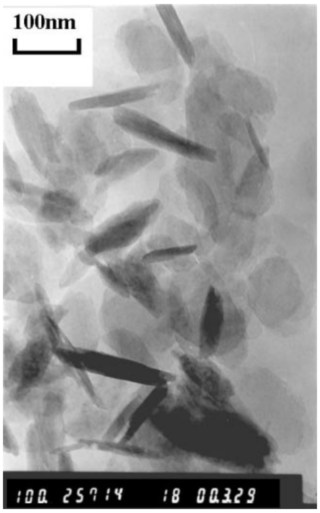

Fig. 2. TEM micrograms of $Mg(OH)_2$ nanocrystals synthesized with high-pressure drying under supercritical ethanol of the $Mg(OH)_2$ alcogel.

Further processing with flowing nitrogen under normal pressure of the $Mg(OH)_2$-AN-270 sample up to 350, 500, and 650°C resulted in dehydration of the hydroxide to form MgO nanocrystals (Fig. 1B) with sizes averaged to 11.7 (MgO-AN-350), 11.5 (MgO-AN-500), and 10.1 nm (MgO-AN-650), respectively (Table 1). This is remarkable since the dehydration up to the temperature as high as 650°C did not cause significant sintering to larger MgO crystals, though the texture structure changed to some extent according to the BET surface areas (Table 1). On the other hand, the dehydration to 500°C by calcinations of sample $Mg(OH)_2$-AS-270 in air led to collapse of the elongate 14 nm × 62 nm crystals to form significantly smaller MgO-AS-500 crystals (ca. 11 nm), which is similar to earlier observations that are ascribed as a "blossoming" behavior in the processing of the methoxide-based sol–gel synthesized $Mg(OH)_2$ [9,13,23,24] and $Ca(OH)_2$ [13] with supercritical drying and high temperature (500°C) dehydration under vacuum. In this present work, however, the "blossoming" also happened during the calcination in air. Apparently shown by the last column of Table 1, the present conventional preparation of MgO-CP-500 also blossomed from its hydroxide precursor ($Mg(OH)_2$-CP-110, 11 nm × 37 nm) to smaller MgO crystals (ca. 8 nm) during the calcinations at 500°C. Also noticeable is that a further processing of the MgO crystallite from both the supercritical and conventional precursors to 650°C in air caused significant sintering to form much larger crystals (ca. 20 nm) that are twice the size of MgO-AN-650. Consequently, the surface areas of MgO-AS-650 and MgO-CP-650 became very much smaller (45 m^2/g) after the calcinations at 650°C, which are also in contrast with the surface area of sample MgO-AN-650 (97.6 m^2/g).

These present data, therefore, demonstrate that normal-pressure processing of the hydroxide alcogel derived from conventional inorganic metal salt is a novel method, coded as AN preparation, for the preparation of small nanocrystallite of MgO. In a separate work to be published later, we have been able to show that this method can be explored as a general method for the preparation of nanocrystals of metal oxides, such as TiO_2 and ZrO_2 [20,21,25]. However, it should be mentioned that the sizes (ca. 10–11 nm) of MgO-AN-500 crystallites are larger and the surface areas much smaller than those (ca. 4.5 nm) synthesized by supercritical drying and vacuum processing at 500°C of the methanol gels derived from $Mg(OCH_3)_2$ [8–12].

3.2. Catalytic application of the nano-MgO

The samples of $Mg(OH)_2$ and MgO nanocrystals were used to support 7.0–9.5 wt.% Ni by impregnation and calcinations at 650°C. The Ni/MgO-AN-270, -AS-270 and -CP-110 samples are prepared with $Mg(OH)_2$-AN-270, -AS-270 and -CP-110, respectively. Ni/MgO-C is a reference sample prepared with a commercial MgO composed of large crystals (50–100 nm). These samples were used as catalysts for the CO_2 reforming of methane to produce syngas. Table 2 gives the physicochemical properties of these catalysts. As shown in Fig. 3, no detectable free NiO-phase exists in the calcined catalysts irrespective of the support preparations, indicating that the nickel ions are incorporated to form solid solutions that are better expressed as $Ni_xMg_{1-x}O$ ($x = 0.16$–0.20).

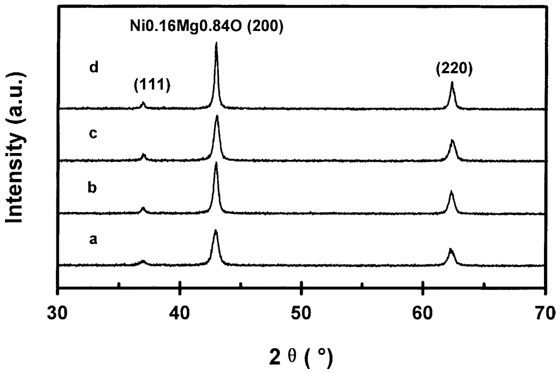

Fig. 3. XRD patterns of the calcined Ni/MgO catalysts: (a) Ni/MgO-AS-270; (b) Ni/MgO-AN-270; (c) Ni/MgO-CP-110; (d) Ni/MgO-C.

TPR experiment revealed no significant reduction of Ni^{2+} ions below 800°C in the Ni/MgO-AS and Ni/MgO-AN samples, but both Ni/MgO-C and Ni/MgO-CP-110 samples showed a distinct reduction peak at 560–750°C, though these samples cannot be

Table 2
Physicochemical properties of the Ni/MgO catalysts

Catalyst	Ni loading[a] (wt.%)	BET surface ($m^2\,g^{-1}$)	Ni phase in the calcined catalyst	Reducibility[b] (%)	Dispersion[c] (%)	Crystal size of the oxide support[d] (nm)
Ni/MgO-AS-270	7.3	45.3	$Ni_{0.16}Mg_{0.84}O$	23.0	12.8	19.8
Ni/MgO-AN-270	9.5	42.6	$Ni_{0.20}Mg_{0.80}O$	21.8	12.6	24.5
Ni/MgO-AN-350	7.1	41.7	$Ni_{0.16}Mg_{0.84}O$	20.9	12.1	25.6
Ni/MgO-CP-110	7.1	45.0	$Ni_{0.16}Mg_{0.84}O$	32.6	11.3	21.0
Ni/MgO-C	7.3	24.0	$Ni_{0.16}Mg_{0.84}O$	25.6	5.5	34.2

[a] Detected by XRF.

[b] Reduction percentage of Ni^{2+} ions measured by TPR up to 860°C followed by another 30 min reduction at this temperature.

[c] Dispersion of the reduced metallic Ni measured by the ratio, 2(area of H_2-TPD-peak)/(area of TPR-peak).

[d] Calculated from (2 0 0) diffraction line of MgO in the reduced catalysts.

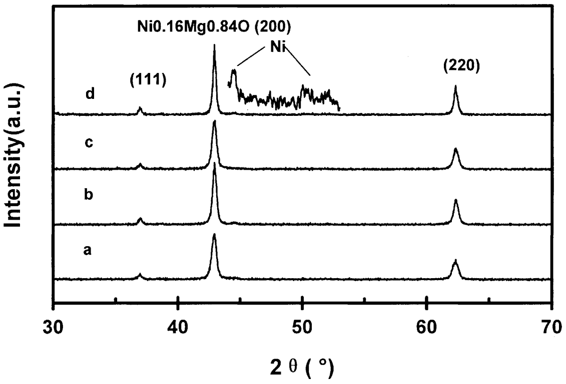

Fig. 4. XRD patterns of the reduced Ni/MgO catalysts: (a) Ni/MgO-AS-270; (b) Ni/MgO-AN-270; (c) Ni/MgO-CP-110; (d) Ni/MgO-C; the inserted amplification of pattern-d shows the presence of Ni metal.

differentiated by their XRD patterns (Fig. 3). According to earlier studies on related catalyst system [26,27], the absence of the reduction signal at 560–750°C suggests that Ni^{2+} ions are completely incorporated into the bulk lattice of MgO in the Ni/MgO-AS and -AN samples, while its presence with the Ni/MgO-C and -CP-110 samples indicates that these two samples contain Ni^{2+} ions in the immediate sub-surface layer.

Since metallic Ni is crucial for the desired catalysis of the CO_2/CH_4 reaction [2–4,18,19,28], the samples were reduced at 850°C, to ensure formation of Ni metal catalyst, before they were tested for the reforming reaction. Fig. 4 shows that the reduced catalysts still hold the feature of the solid solution; only a small part of Ni^{2+} ions is reduced as indicated by the amplified part of pattern-d. Reducibility of Ni^{2+} ions in the calcined samples and dispersion of the reduced Ni metal after the reduction at 850°C are listed in Table 2. Also given in this table are the overall BET surface areas and the crystallite sizes of the oxide solution supports. The properties of all the samples except Ni/MgO-C, which shows significant lower surface area and metal dispersion but much larger support crystals, seem similar to each other.

Fig. 5 shows the catalytic activity of Ni/MgO catalysts by conversions of methane and CO_2, respectively. Comparable conversions for both reactants confirm that Ni-supported MgO is the ideal chemical catalyst for the dry reforming of methane as shown by the high selectivity for CO (>95%) and other selectivity parameters presented in Table 3. Ni/MgO-C prepared with the commercial oxide showed little activity and deactivated quickly. The activity of the conventional preparation Ni/MgO-CP-110 catalyst seems not stabilized in the 100 h tested. Noticeably, $Mg(OH)_2$ support from the alcogel precursor either by supercritical processing or normal-pressure processing in nitrogen atmosphere produces Ni/MgO-AS-270 or Ni/MgO-AN-270 catalyst of the highest activity and catalytic stability. The conversions of both reactants (ca. 88–91%) reached their equilibrium values (ca. 87% at 750°C). Importantly, we found that the Ni/Mg-AS-270 and -AN-270 catalysts have excellent anti-carbon property; these two catalysts did not sign any carbon deposition since their color did not change even a little after being used for up to 100 h in the reaction.

Since both Ni/MgO-AS-270 and Ni/MgO-AN-270 catalysts are prepared by impregnation of $Mg(OH)_2$ with nickel. It is in question that whether highly active and stable anti-carbon Ni/MgO catalyst can be developed by direct impregnation of nickel onto the nanosized MgO, instead of $Mg(OH)_2$. This is answered positively by a direct use of MgO-AN-350 (11–12 nm, Table 1) as support of the Ni catalyst. This catalyst is coded as Ni/MgO-AN-350; its physicochemical properties are given by a row in the middle of Table 2. Fig. 6 shows the activity of this catalyst with the methane conversion data. Activity and product selectivity of this catalyst are also compared with the other catalysts in Table 3. It is clear from Fig. 6 that this Ni/MgO-AN-350 catalyst shows very stable catalytic activity even after unusually experiencing a wide range of changing reaction conditions, such as jumping the temperature between 700 and 800°C and fluctuating the feed space velocity between 10^4 and 10^5 ml/(h g_{cat}). Since the normal reaction temperature (757°C) is lower than those (800–850°C) used in most literature reports [2–4], the present Ni/MgO-AN catalysts seem to possess higher activity than those reported in the literature for most Ni/MgO catalysts of various preparations. Few catalysts were reported to give 90% methane or CO_2 conversion even at above 800°C, in comparison the present Ni/MgO-AN-350 renders 93–94% methane conversion at 800°C (Fig. 6).

In conclusion, the present work provides a novel and convenient synthetic approach for producing nanocrystals of MgO by use of conventional sol–gel

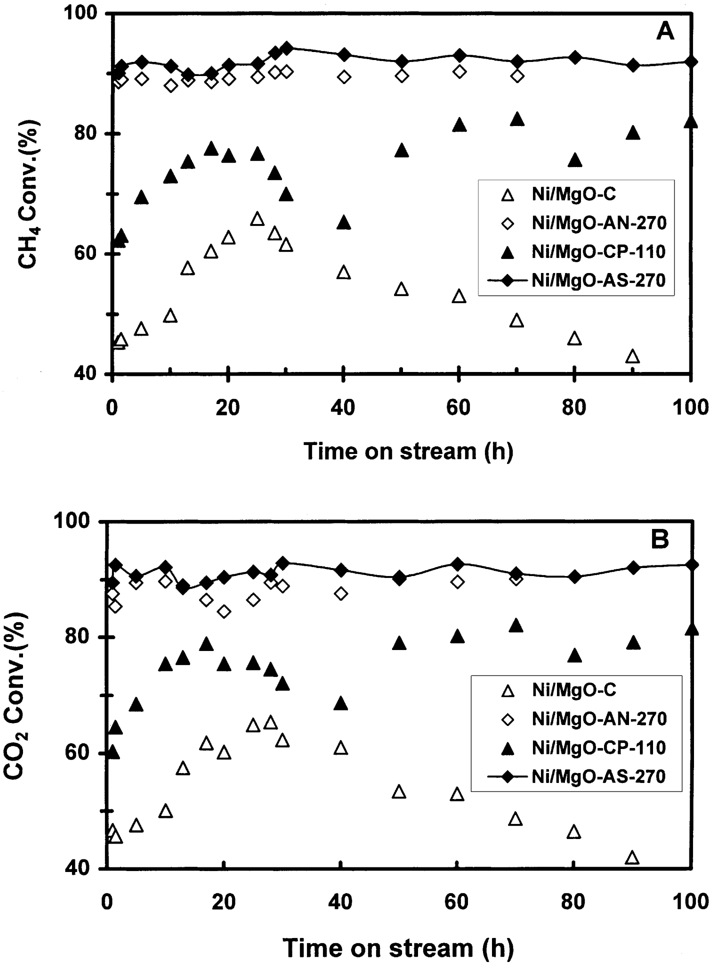

Fig. 5. Time courses for: CH_4 (A); CO_2 (B) conversions over Ni/MgO catalysts at 757°C.

Table 3
Activity and selectivity of different Ni/MgO catalysts averaged for a reaction period of TOS = 70 h[a]

Catalyst	CH_4 conversion (%)	CO_2 conversion (%)	TOF CH_4 (s^{-1})	CO selectivity (%)	H_2 selectivity (%)	Average CO/H_2 (molar ratio)	Average CO/H_2O	Average $CO/(H_2 + H_2O)$
Ni/MgO-AS-270	91.2	92.1	3.6	99.5	82.9	1.2	11.0	1.06
Ni/MgO-AN-270	88.0	89.7	3.4	100	90.9	1.1	26.4	1.02
Ni/MgO-AN-350	90.0	89.5	3.5	98.7	89.7	1.1		
Ni/MgO-CP-110	73.0	75.4	2.4	97.8	88.9	1.1		
Ni/MgO-C	49.8	50.1	2.1	94.7	90.2	1.1	30.0	0.96

[a] Reaction conditions: $T = 757°C$, $P = 1$ atm, $CO_2/CH_4 = 1$, GHSV $= 2.4 \times 10^4$ ml/(g_{cat} h).

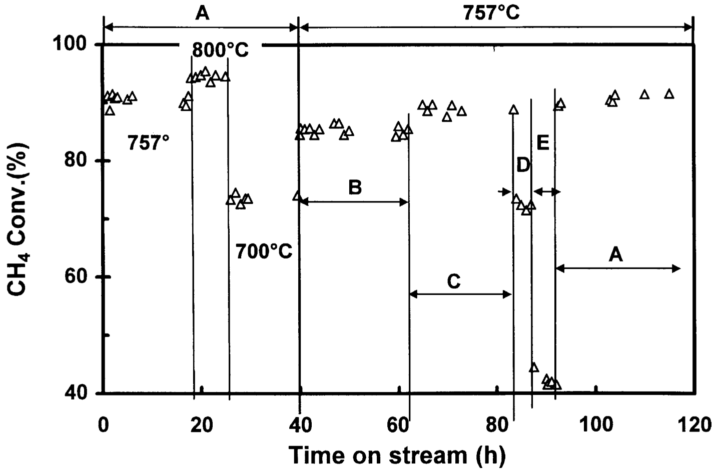

Fig. 6. Response of CH_4 conversion over Ni/MgO-AN-350 catalyst under different reaction conditions: the reaction temperature is indicated above the figure; the capital letter-marks refer to reaction space velocity of GHSV: 2.4×10^4 (A); 3.6×10^4 (B); 4.8×10^4 (C); 7.2×10^4 (D); 9.6×10^4 ml/(h g_{cat}) (E).

chemistry of inorganic chloride. This approach also avoids using high-pressure supercritical condition to process $Mg(OH)_2$ alcogel, instead, it uses normal-pressure nitrogen to process the alcogel. MgO nanocrystals (10–12 nm) thus prepared are able to withstand the "sintering" up to 650°C. Ni/MgO catalyst prepared with either $Mg(OH)_2$ or MgO nanocrystals from the novel preparation gives primary promising results for the development of highly efficient and long-term catalyst for the CO_2 reforming of methane.

Acknowledgements

The authors are indebted to Profs. J.L. Li and Z.X. Cheng for helpful discussion. This work was financially supported by grants from NSFC (Grant 20073023) and the Fundamental Research Foundation of Tsinghua University (Grant 1999051).

References

[1] H. Hattori, Chem. Rev. 95 (1995) 537.
[2] Y.H. Hu, E. Ruckenstein, Catal. Lett. 43 (1997) 71.
[3] E. Ruckenstein, Y.H. Hu, Appl. Catal. A 154 (1997) 185.
[4] K. Tomishige, O. Yamazaki, Y. Chen, K. Yokoyama, X. Li, K. Fujimoto, Catal. Today 45 (1998) 35.
[5] D. Dyrssen, D.R. Turner, in: J. Paul, C.M. Pradier (Eds.), Carbon Dioxide Chemistry: Environmental Issues, Athenaeum Press, Cambridge, 1994, p. 317.
[6] S.J. Teichner, G.A. Nicolaon, M.A. Vicarini, G.E. Gardes, Adv. Colloid Interf. Sci. 5 (1976) 245.
[7] Chem. Rev. 90 (1990) 33.
[8] Y.X. Li, K.J. Klabunde, Langmuir 7 (1991) 1388.
[9] S. Utamapanya, K.J. Klabunde, J.P. Schlup, Chem. Mater. 3 (1991) 175.
[10] K.J. Klabunde, J.V. Stark, O. Koper, C. Mohs, D.G. Park, S. Decker, Y. Jiang, I. Lagadic, D. Zhang, J. Phys. Chem. 100 (1996) 12142.
[11] J.V. Stark, D.G. Park, I. Lagadic, K.J. Klabunde, Chem. Mater. 8 (1996) 1904.
[12] J.V. Stark, K.J. Klabunde, Chem. Mater. 8 (1996) 1913.
[13] O.B. Koper, I. Lagadic, A. Volodin, K.J. Klabunde, Chem. Mater. 9 (1997) 2468.
[14] H.-W. Xiang, B. Zhong, S.-Y. Peng, Ranliao Huaxue Xuebao (Chin. J. Fuel Chem.) 22 (1994) 119.
[15] H.-W. Xiang, B. Zhong, S.-Y. Peng, Ranliao Huaxue Xuebao (Chin. J. Fuel Chem.) 22 (1994) 125.
[16] H.-W. Xiang, B. Zhong, S.-Y. Peng, Fezi Cuihua (Chin. J. Mol. Catal.) 8 (1994) 263.
[17] H.-W. Xiang, B. Zhong, S.-Y. Peng, Catal. Today 30 (1996) 183.
[18] J.-M. Wei, B.-Q. Xu, J.-L. Li, Z.-X. Cheng, Q.-M. Zhu, Appl. Catal. A 196 (2000) L167.
[19] J.-M. Wei, B.-Q. Xu, Z.-X. Cheng, J.-L. Li, Q.-M. Zhu, Stud. Surf. Sci. Catal. 130 (2000) 3687.
[20] B.-Q. Xu, J.-M. Wei, S.-F. Ying, X. Zhang, Q.M. Zhu, Chinese Patent, Application No. 00100554.5 (2000).
[21] B.-Q. Xu, J.-M. Wei, F.-Z. Zhang, Q.-M. Zhu, Chinese Patent, Application No. 00106166.6 (2000).

[22] W.B. Innes, in: R.B. Anderson (Ed.), Experimental Methods in Catalytic Research, Academic Press, New York, 1968, p. 44.
[23] O.B. Koper, K.J. Klabunde, Chem. Mater. 5 (1993) 500.
[24] J. Dewing, G.T. Monks, B. Youll, J. Catal. 44 (1976) 226.
[25] B.-Q. Xu, J.-M. Wei, S.-F. Ying, J.L. Li, Z.X. Cheng, in preparation.
[26] G.C. Bond, S.P. Sarsam, Appl. Catal. 38 (1988) 365.
[27] J.G. Highfield, A. Bossi, F.S. Stone, in: G. Poncelet, P. Grange, P.A. Jacobs (Eds.), Preparation of Catalysts III, Elsevier, Amsterdam, 1983, p. 181.
[28] M.C.J. Bradford, M.A. Vannice, Catal. Rev. Sci. Eng. 41 (1999) 1.